Optica Applicata, Vol. XXXVI, No. 2–3, 2006

High resolution and analytical electron microscopy of ZnO layers doped with magnetic ions for spintronic applications

M. ABOUZAID[1], P. RUTERANA[1*], C. LIU[2], H. MORKOÇ[2]

[1]SIFCOM UMR 6176 CNRS-ENSICAEN, 6, Boulevard du Marechal Juin, 14050 Caen Cedex, France

[2]Department of Electrical Engineering, Virginia Commonwealth University, Richmond, VA 23284, USA

[*]Corresponding author: P. Ruterana, pierre.ruterana@ensicaen.fr

We have investigated the effect of temperature on the crystalline quality of (Zn, Mn)O thin films prepared by rf magnetron sputtering using *c*-plane sapphire substrates. The layers comprised an Mn doped part towards the surface on top of about a 150 nm pure ZnO layer. They exhibit a columnar structure depending on the deposition temperature; the adjacent domains are rotated from one another by 90°, putting $[10\bar{1}0]$ and $[11\bar{2}0]$ directions face to face. At high Mn concentration this columnar structure is blurred by the formation of Mn rich precipitates for which we report on the structure, composition and crystallographic relationships with the surrounding matrix.

Keywords: ZnO, transmission electron microscopy, ferromagnetism, manganese doping, spintronics, sputtering, Mn rich precipitates.

1. Introduction

Transition-metal-doped ZnO is attracting the attention of researchers as a promising diluted magnetic semiconductor (DMS) material for its use in spintronics. Based on the prediction of DIETL *et al.* [1], considerable effort has been focused on achieving reliable ZnO-based DMS with a Curie temperature above room temperature by doping with transition metals [2], especially Mn [3] and Co [4]. Ferromagnetism has been reported in insulating (Zn, Mn)O [5], *n*-type (Zn, Mn)O [3], and *p*-type (Zn, Mn)O. However, doping ZnO layers with these transition metal atoms may lead to the formation of various interphase precipitates, which may have magnetic properties [6]. A considerable number of thin film deposition techniques are now available for the production of good quality ZnO layers. The most common technology used for depositing ZnO films is laser ablation [7]. Metalorganic chemical vapour deposition (MOCVD) [8–10] is an alternate technique for growth, whose advantages

lie its chemistry and thermodynamic dependent growth, control at the atomic level, large area deposition, and the possibility of different *in situ* doping processes. Typical growth conditions are as follows: chamber pressure of 20–50 torr, a growth temperature of 250– 600°C [11]. Such ZnO layers grown on sapphire were shown to have a relatively low thermal stability after annealing at about 800°C [11]. Molecular beam epitaxy (MBE) technique is also currently used for the growth of high quality ZnO [12].

It is also claimed that in ZnO, ferromagnetism may be connected with *p*-doping especially using nitrogen. One of the easiest and low cost methods for introducing high doses of nitrogen may be deposition by rf sputtering [13]. In this technique incorporation of nitrogen is done directly in the plasma and large amount can be incorporated in the layer in contrast with the other growth techniques such as MBE or MOCVD. However, the deposited layers may be of poorer crystalline quality and the existence of structural imperfections can impede the clarification of experimentally observed ferromagnetism in DMS materials. Therefore, our aim is to provide a better understanding of the observed magnetic behaviour by carrying out a detailed microstructural analysis of rf transition metal and nitrogen-doped ZnO thin films.

In this transmission electron microscopy investigation, it is pointed out that the substrate temperature during deposition plays an important role for the layer microstructure.

2. Experimental

The ZnO buffer layer was deposited at 650°C and the Mn-doped ZnO film was deposited within the 500 to 750°C temperature range. An rf power of 150 W was used to sputter the ZnO target. The DC power applied to the Mn target was 5 W for the Mn-doped ZnO film. The targets were pre-sputtered for 5 minutes before the actual deposition to remove contamination from the target surface. The as-deposited films were annealed at 850°C for 1 hour in the air ambient in order to improve the crystalline quality. The substrates were either sapphire or thick GaN buffer layers; the deposition conditions are summarized in Tab. 1.

T a b l e 1. Deposition temperature, substrate and doping of the samples (*a* and *na* stand for annealed and non-annealed, respectively).

Sample	Substrate	T [°C]	N (rf power, watt)
Sp 105	Sapphire	550	0
Sp 110	Sapphire	650	10
Sp 272	GaN	750	0
Sp 280	GaN	550	10
Sp 316	GaN	500	0
Sp 318*na*	Sapphire	500	10
Sp 318*a*	Sapphire	500	10

Cross-sectional TEM samples were prepared by gluing two pieces of the film face to face, cutting to slices followed by mechanical polishing down to100 μm and then dimpling to 10 μm. The electron transparency was finally obtained by ion-milling with the sample holder kept at liquid nitrogen in order to minimize the irradiation damage. The observations were carried out with 002B Topcon high resolution microscope operated at 200 kV.

3. Results

In the following, we first discuss the influence of the deposition temperature on the sputtered ZnO crystalline structure, next, we present the results on the various phases that form upon doping the layers with Mn.

3.1. Influence of the deposition temperature

The first observation is great influence of the deposition temperature on the layer microstructure, especially on sapphire, at the highest temperatures (650°C), the layers exhibited a strong columnar growth, with large adjacent columns (diameter >200 nm) of different orientations as can be noticed in the bright field micrograph of Fig. 1 in which the dark columns are imaged along the $[11\bar{2}0]$ axis of ZnO. When the deposition temperature is lowered to 550°C, the columnar growth is still present, but the column diameter is strongly decreased, the size of the individual columns is below 50 nm (Fig. 2**a**). As recorded along the $[10\bar{1}0]$ zone axis of sapphire, the diffraction pattern (Fig. 2**b**) in an area containing many columns in ZnO exhibits two zone axes, *i.e.*, the $[10\bar{1}0]$ and $[11\bar{2}0]$. Therefore, the two main epitaxial relationships in mismatched growth of wurtzite structures, which have been reported on the growth of wurtzite GaN on the [0001] sapphire surface [14], coexist in this instance and adjacent columns can be rotated, one from the other, through 90° around the [0001] direction.

After annealing, the magnetization was measured and a substantial effect was obtained in practically all these layers. In the micrograph of Fig. 2**a**, the Mn-doping was 10%; and the doping was started after the deposition of about 150 nm. This figure points to a clear structural difference between the doped and undoped areas. The undoped region exhibits a columnar growth whereas the doped area contains

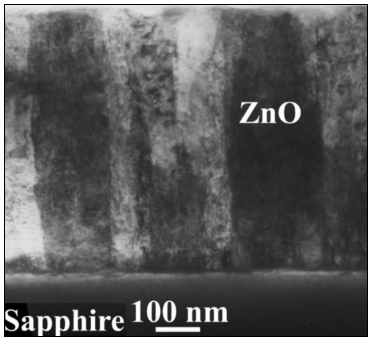

Fig. 1. Large columns after deposition at 650°C.

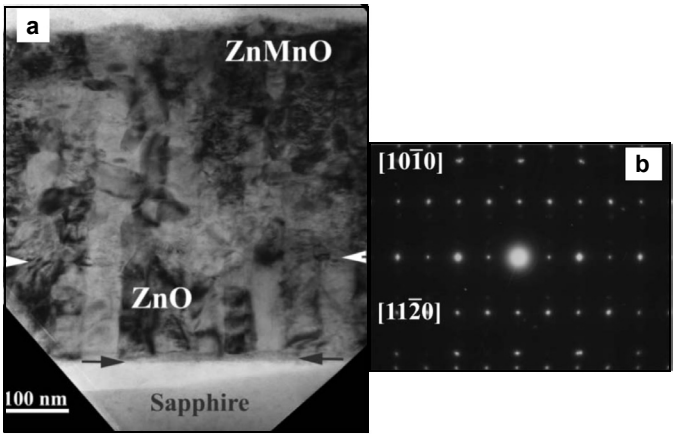

Fig. 2. Layer deposited at 550°C, (**a**) rough interface to the Mn-doped area towards the surface, and an intermediate phase at the sapphire surface; (**b**) a diffraction pattern of a large area showing the two epitaxial relationships of the columns; the two coexisting zone axis are marked.

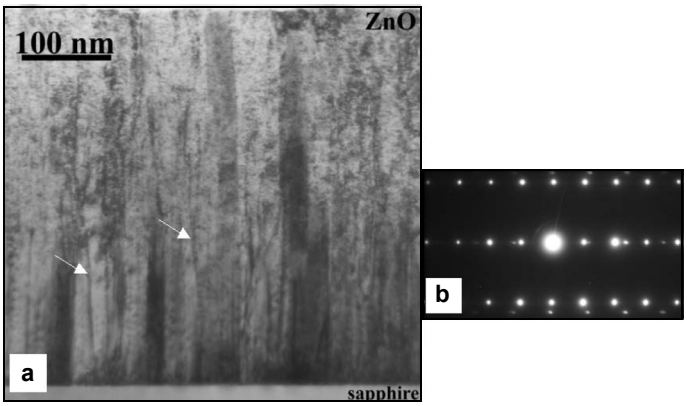

Fig. 3. Deposition at 500°C: the layers exhibit a mosaic growth (**a**); only one epitaxial relationship is present (**b**).

a large number of precipitates of various shapes and sizes, which blur out the columnar structure. The interface between the two areas is very rough as indicated by the two white arrows. The peak-to-peak roughness is about 40 nm substantially larger than at the top surface of the Zn(Mn)O layer. This may imply that there has been interdiffusive reaction in this area, either during the deposition or the subsequent annealing step, which took place at 800°C. At the interface with the sapphire substrate (see black arrows), there is a thin layer, which exhibits a different contrast, and this is also the case for the layers deposited at 650°.

When the deposition temperature is lowered down to 500°C, the misorientation between the growth domains becomes very small, the epitaxial relationship which

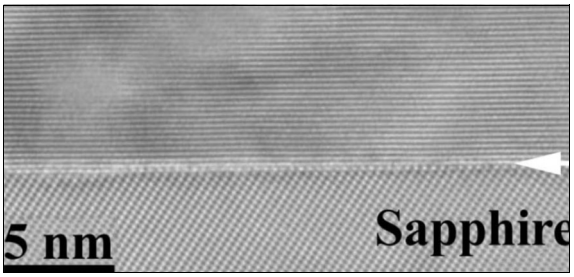

Fig. 4. High resolution micrograph of the interfacial area with the sapphire substrate.

dominates the growth on (0001) sapphire also for GaN is the only one to take place [15]. The layers end up with a mosaic growth mode (Fig. 3**a**) as has already been pointed out in GaN layers grown on top of sapphire [16] and only one epitaxial relationship is exhibited: $[0001]_{Sap}//[0001]_{ZnO}$ and $[10\bar{1}0]_{Sap}//[11\bar{2}0]_{ZnO}$ (Fig. 3**b**); the adjacent columns are now bounded by threading dislocations, some of them are shown by arrows in Fig. 3**a**.

At the interface with the sapphire substrate, the ZnO layer has now grown directly, there is no intermediate phase as in samples deposited at higher temperatures. In this high resolution TEM image, the sapphire substrate is viewed along the $[11\bar{2}0]$ zone axis. The transition between sapphire and ZnO takes place within one atomic layer as shown by the white arrow (Fig. 4).

T a b l e 2. Columnar growth and interfacial phase formation versus the deposition temperature.

T/Sub [°C]	Sapphire [nm]	Interphase
650	200	Yes
550	60	Yes
500	~10	No

So, as far as the ZnO layer quality is concerned within the temperature range under investigation, it appears that the best growth condition is attained at the lowest temperature of 500°C. At this temperature (Tab. 2), there is no more columnar growth and no interfacial phase is formed. In addition, this indicates that the interfacial phase has formed during the deposition and not in the subsequent step of annealing at 800°C.

3.2. Interphase

A micrograph of the interfacial phase, which is formed in the high temperature layers, is exhibited in Fig. 5. As can be noticed, the thickness of this layer is not constant, it can vary from 2 to 5 nm. However, one point is quite obvious, there is a noticeable difference between its two interfaces. The ZnO/interphase side is abrupt within one atomic layer, whereas the interphase/sapphire interface extends to a few monolayers. This is a possible indication that the reaction which leads to its formation may have

proceeded from ZnO towards sapphire. Moreover, all over this layer, one family of lattice fringes is parallel to the (0001) sapphire. In this area, we have a crystalline phase, which is viewed along a low index zone axis. As can be seen in Fig. 6, two families of lattice planes are present in this highly magnified part of the same image

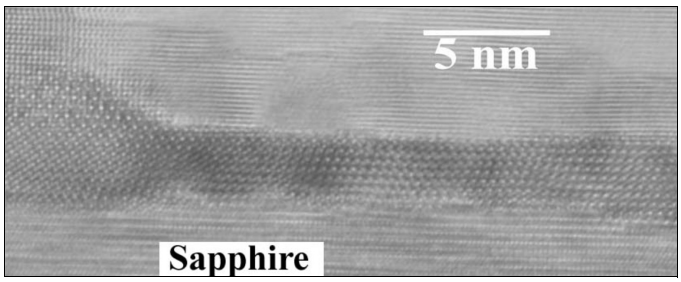

Fig. 5. High resolution micrograph of the interfacial phase in 550° ZnO on (0001) sapphire.

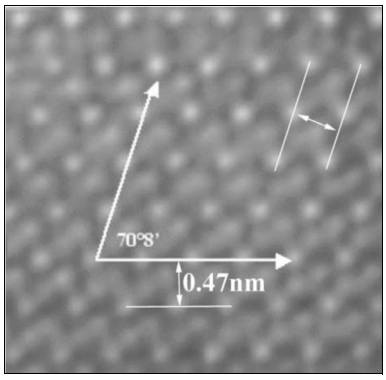

Fig. 6. High magnification image of the interfacial phase with *d* spacing and angles.

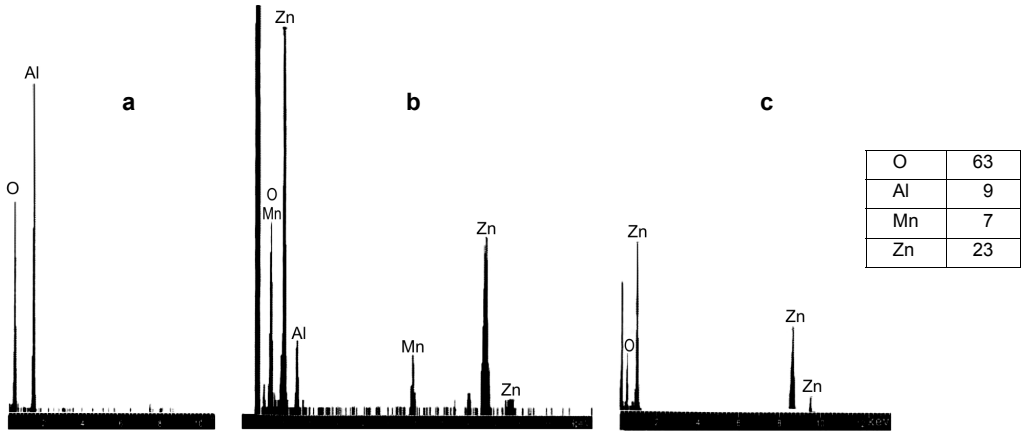

O	63
Al	9
Mn	7
Zn	23

Fig. 7. EDS analysis of the interfacial area: 6 nm inside sapphire (**a**), on top of the interphase (**b**), 6 nm inside the ZnO (**c**).

and they have the same d spacing as well as making an angle of 70°. This is a good indication that this interphase is most probably cubic.

We have carried out EDS analysis in the interfacial area using a beam diameter of about 3 nm; the various spectra are shown in Fig. 7. The spectra were recorded just on top of the interphase and at about 6 nm on each side. They show clearly that at this scale, there is negligible interdiffusion between sapphire and ZnO (see Figs. 7**a** and 7**c**).

The most striking observation is that this interphase layer contains Mn. This means that during the deposition, Mn has diffused from the doped area (150 nm) and come to react at the interface with sapphire. In the first 100–150 nm undoped ZnO, independent of the position, we have not been able to detect any Mn. It is then possible that there has been some driving force for the reaction to take place at the interface only. In Figure 7, we have inserted the deduced atomic composition of this phase. Although, the error bars are difficult to estimate and can be important, mainly due to our experimental set up, this analysis is an indication that this compound may be a trimetallic oxide with roughly the same amount of Mn and Al.

3.3. Precipitates inside Mn-doped areas

As can be seen in Fig. 8, numerous precipitates are present inside the Mn containing areas particularly in the layer doped at 10%. They have various shapes and sizes and can be as large as a few 100 nm. Some may be elongated in the basal plane (black arrows) and others may be more or less round shaped (white arrows). As the round shaped ones are mostly of large size, we have been able to identify their structure and composition using EDS and HRTEM.

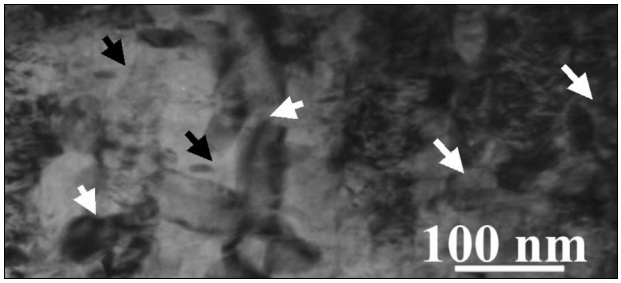

Fig. 8. Precipitation in 10% Mn-doped ZnO layer, arrows show some of the precipitates.

A typical HRTEM image of a round shaped precipitate is shown in Fig. 9, at this scale, the interface of the precipitate with the surrounding matrix is formed by well defined crystallographic facets in the form of ledges separated by steps (arrows).

From Figure 9, we can extract a number of data and useful information on the precipitate and its crystallographic relationship with the surrounding ZnO matrix. The typical angles of 110° between two equivalent directions and 90° between two others allow us to identify the [110] zone axis of a cubic structure. In reference to

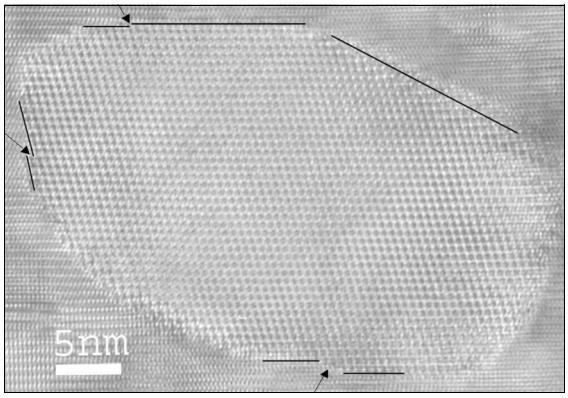

Fig. 9. High resolution TEM micrograph of a typical cubic precipitate viewed along the [110] zone axis.

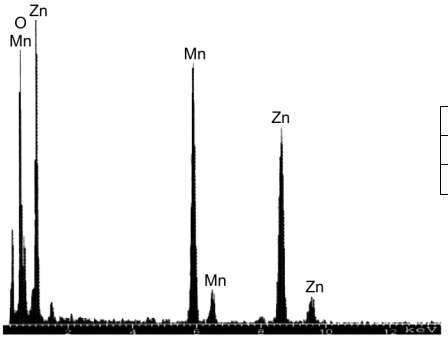

O	61
Mn	21
Zn	19

Fig. 10. EDS analysis of the cubic precipitates and atomic composition of the round shaped cubic precipitate.

the surrounding ZnO matrix, we measured $d_{111} = 4.95$ Å and $d_{220} = 2.98$ Å within 0.1 Å error. We also see clearly that one set of the (111) planes is parallel to type (0001) basal planes of ZnO. EDS analysis (fig.10) of this precipitate gives a $ZnMnO_3$ stoichiometry which agrees with these lattices d spacing within the 0.1 Å errors as stated above. So, this precipitate is of a cubic system with $a = 8.35$ and $d_{111} = 4.83$ Å. Along the [0001] ZnO direction, the formation of such precipitates needs the accommodation of quite a large mismatch (7%).

4. Conclusions

The microstructure of Mn doped ZnO layers obtained by rf sputtering on (0001) sapphire is presented. It is shown that at the optimum deposition temperature investigated, the most common epitaxial growth of ZnO takes place on (0001

sapphire). At higher temperatures, the Mn-doped ZnO layer exhibited a high density of round-shaped cubic and elongated MnZn oxide precipitates. In addition, a trimetallic $(AlMn)ZnO_3$ phase formed in the ZnO/sapphire interface region. The round shaped precipitates are $ZnMnO_3$; they are facetted with extended (0001) ledges and coherent areas in between misfit dislocations along the *c*-direction of the ZnO matrix. The other type of precipitates is elongated inside the ZnO basal plane with almost the same *c* lattice distance. In such heavily Mn doped layers a magnetic effect has been measured, almost in parallel with the formation of the precipitates. For the time being, investigation is still under way in order to determine whether the two effects are correlated. It is clear, even if the precipitates were not magnetic themselves, that their formation may modify the local properties of the doped matrix.

References

[1] DIETL T., OHNO H., MATSUKURA F., CIBERT J., FERRANT D., *Zener model description of ferromagnetism in zinc-blende magnetic semiconductors*, Science **287**(5455), 2000, pp. 1019–22.

[2] PEARTON S.J., NORTON D.P., IP K., HEO Y.W., STEINER T., *Recent advances in processing of ZnO*, Journal of Vacuum Science and Technology B: Microelectronics and Nanometer Structures **22**(3), 2004, pp. 932–48.

[3] HEO Y.W., IVILL M.P., IP K., NORTON D.P., PEARTON S.J., KELLY J.G., RAIRIGH R., HEBARD A.F., STEINER T., *Effects of high-dose Mn implantation into ZnO grown on sapphire*, Applied Physics Letters **84**(13), 2004, pp. 2292–4.

[4] YOON S.W., CHO S.-B., WE S.C., YOON S., SUH B.J., SONG H.K., SHIN Y.J., *Magnetic properties of ZnO-based diluted magnetic semiconductors*, Journal of Applied Physics **93**(10), 2003, pp. 7879–81.

[5] JUNG S.W., AN S.-J., YI G.-C., JUNG C.U., LEE S.-I., CHO S., *Ferromagnetic properties of $Zn_{1-x}Mn_xO$ epitaxial thin films*, Applied Physics Letters **80**(24), 2002, pp. 4561–3.

[6] PEARTON S.J., ABERNATHY C.R., NORTON D.P., HEBARD A.F., PARK Y.D., BOATNER L.A., BUDAI J.D., *Advances in wide bandgap materials for semiconductor spintronics*, Materials Science and Engineering R: Reports **R40**(4), 2003, pp. 137–68.

[7] SRIKANT V., SERGO V., CLARKE D.R., *Epitaxial aluminum-doped zinc oxide thin films on sapphire. I. Effect of substrate orientation*, Journal of the American Ceramic Society **78**(7), 1995, pp. 1931–4.

[8] ROTH A.P., WILLIAMS D.F., *Properties of zinc oxide films prepared by the oxidation of diethyl zinc*, Journal of Applied Physics **52**(11), 1981, pp. 6685–92.

[9] COCKAYNE B., WRIGHT P.J., *Metalorganic chemical vapour deposition of wide band gap II-VI compounds*, Journal of Crystal Growth **68**(1), 1984, pp. 223–30.

[10] GORLA C.R., EMANETOGLU N.W., LIANG S., MAYO W.E., LU Y., WRABACK M., SHEN H., *Structural, optical, and surface acoustic wave properties of epitaxial ZnO films grown on (011 2) sapphire by metalorganic chemical vapor deposition*, Journal of Applied Physics **85**(5), 1999, pp. 2595–602.

[11] JONES A.C., RUSHWORTH S.A., AULD J., *Recent developments in metalorganic precursors for metalorganic chemical vapour deposition*, Journal of Crystal Growth **146**(1–4), 1995, pp. 503–10.

[12] VIGUE F., VENNEGUES P., DEPARIS C., VEZIAN S., LAUGT M., FAURIE J.-P., *Growth modes and microstructures of ZnO layers deposited by plasma-assisted molecular-beam epitaxy on (0001) sapphire*, Journal of Applied Physics **90**(10), 2001, pp. 5115–19.

[13] LIU C., YUN F., XIAO B., CHO S.-J., MOON Y.T., MORKOÇ H., ABOUZAID M., RUTERANA P., YU K.M., WALUKIEWICZ W., *Structural analysis of ferromagnetic Mn-doped ZnO thin films deposited by radio frequency magnetron sputtering*, Journal of Applied Physics **97**(12), 2005, p. 126107.

[14] ÖZGÜR Ü., TEKE A., LIU C., CHO S.-J., MORKOÇ H., EVERITT H.O., *Stimulated emission and time -resolved photoluminescence in rf-sputtered ZnO thin films*, Applied Physics Letters **84**(17), 2004, pp. 3223–5.
[15] DOVIDENKO K., OKTYABRKY S., NARAYAN J., RAZEGHI M., *Aluminum nitride films on different orientations of sapphire and silicon*, Journal of Applied Physics **79**(5), 1996, pp. 2439–45.
[16] PONCE F.A., *Defects and interfaces in GaN epitaxy*, MRS Bulletin **22**(2), 1997, pp. 51–7.

Received December 15, 2005